Title

Probing the energetics of organic–nanoparticle interactions of ethanol on calcite

Journal

Proceedings of the National Academy of Sciences of the United States of America, 112(17)

ISSN

0027-8424

Authors

Wu, Di

Navrotsky, Alexandra

Publication Date

2015-04-28

DOI

10.1073/pnas.1505874112

Peer reviewed

Probing the energetics of organic–nanoparticle interactions of ethanol on calcite

Di Wu and Alexandra Navrotsky[1]

Peter A. Rock Thermochemistry Laboratory and Nanomaterials in the Environment, Agriculture, and Technology Organized Research Unit, University of California, Davis, CA 95616

Contributed by Alexandra Navrotsky, March 25, 2015 (sent for review November 3, 2014)

Knowing the nature of interactions between small organic molecules and surfaces of nanoparticles (NP) is crucial for fundamental understanding of natural phenomena and engineering processes. Herein, we report direct adsorption enthalpy measurement of ethanol on a series of calcite nanocrystals, with the aim of mimicking organic–NP interactions in various environments. The energetics suggests a spectrum of adsorption events as a function of coverage: strongest initial chemisorption on active sites on fresh calcite surfaces, followed by major chemical binding to form an ethanol monolayer and, subsequently, very weak, near-zero energy, physisorption. These thermochemical observations directly support a structure where the ethanol monolayer is bonded to the calcite surface through its polar hydroxyl group, leaving the hydrophobic ends of the ethanol molecules to interact only weakly with the next layer of adsorbing ethanol and resulting in a spatial gap with low ethanol density between the monolayer and subsequent added ethanol molecules, as predicted by molecular dynamics and density functional calculations. Such an ordered assembly of ethanol on calcite NP is analogous to, although less strongly bonded than, a capping layer of organics intentionally introduced during NP synthesis, and suggests a continuous variation of surface structure depending on molecular chemistry, ranging from largely disordered surface layers to ordered layers that nevertheless are mobile and can rearrange or be displaced by other molecules to strongly bonded immobile organic capping layers. These differences in surface structure will affect chemical reactions, including the further nucleation and growth of nanocrystals on organic ligand-capped surfaces.

thermodynamics | adsorption calorimetry | ligand-capped nanocrystal | biomineralization | carbonate formation

The interactions between simple organic molecules and inorganic surfaces, nanoparticles (NP), and clusters with controlled properties provide fundamental insights to understand much more complicated natural phenomena, including biomineralization (1), contaminant and nutrient transport in soils and aquifers (2), and CO_2 transport and carbonate formation (3–5). Such organic–inorganic systems are also encountered in technological environments, particularly selective catalysis (6–8), enhanced oil recovery (9), self-assembly of colloidal NPs (10–13), and CO_2 capture and sequestration (14). Despite being well-documented qualitatively, the magnitudes of such interactions and their impact on the interface molecular configurations have barely been directly identified. In this context, NP plays a very active and crucial role linking the organic and inorganic worlds. Their high surface energies enable ready assembly with organic molecules (15). Such organic termination or capping may mask the original NP surface identity (4) (hydrophobicity, charge, and/or chemical group), resulting in a modified outer shell, which may feature unique configuration and functionality (electronic, optical, steric, and/or chemical) (1, 5, 16). However, a clear understanding of the organic ligand–NP interactions and surface chemistry–structure relations is still far from complete.

Thorough thermodynamic study of the energetics of organic ligand capping of NPs is essential to understanding reactivity. Herein, we use calcite NPs with ethanol, as simple chain-like polar molecule, as representative of hydroxyl containing organic ligands. Calcite is the most stable calcium carbonate polymorph (17), well known for its ability to form numerous multifunctional nanoscale architectures with proteins made by organisms (18, 19). Previous studies by molecular dynamics (MD), density functional theory (DFT), and atomic force microscopy (AFM) suggest that, once adsorbed, ethanol molecules self-assemble to a highly ordered monolayer on the calcite surface (20, 21). A low ethanol density, spatially thin gap between the first and second layer of adsorbed ethanol is also predicted to exist (22). However, so far, no direct experimental evidence describes the energetics of such a unique surface configuration.

Direct gas adsorption calorimetry was initially developed in our laboratory to measure the hydration enthalpy of NPs (23, 24). The experimental system includes a commercial gas adsorption analyzer coupled with a microcalorimeter (25). Recently, we have expanded its application to multiple gases, including CO_2, Kr, and Xe (26–28), on metal–organic frameworks. In this work, to explore the nature of organic ligand–NP interactions, ethanol vapor was used as the adsorbate, whereas a series of nanophase calcite particles was selected to represent a nanoscale inorganic material. The results show a complex pattern of adsorption energetics which lends support to the structural model proposed by computational and microscopic methods (20–22).

Four high-quality commercial nanocalcite samples, characterized and used previously in a study of calcite surface energy (29), were used as adsorbents (Table S1). The details of direct gas adsorption calorimetry experiments are described in *Materials and Methods*.

Results

The properties of the nanocalcites (same materials as used in our previous study of surface energy) are listed in Table S1 (29). All samples have highly uniform particle size (65–133 nm). This range of sizes provides the necessary large surface areas for adsorption calorimetry, maintaining a recognizable calcite structure, while avoiding significant structural disruption from high concentration

Significance

Organic ligand–inorganic nanoparticle (NP) interactions are crucial in both natural and engineering conditions. This paper reports a rich energetics of organic–NP binding as a function of molecular coverage for ethanol–nanocalcite system. A stepwise, yet gradually and continuously evolved energetics from weak associating to strong bonding to classical capping is revealed. Such information may reinforce our understanding of complex phenomena at organic–NP interfaces, and may also aid exploratory material scientists by providing solid, fundamental thermodynamic insights.

Author contributions: D.W. and A.N. designed research; D.W. performed research; D.W. and A.N. analyzed data; and D.W. and A.N. wrote the paper.

The authors declare no conflict of interest.

[1]To whom correspondence should be addressed. Email: anavrotsky@ucdavis.edu.

This article contains supporting information online at www.pnas.org/lookup/suppl/doi:10.1073/pnas.1505874112/-/DCSupplemental.

of surface defects and/or amorphization. Additionally, there are no detectable adsorbed organic species (infrared spectroscopy) or phase transitions (powder X-ray diffraction) after pretreatment at 150 °C under vacuum (29). Therefore, the signals monitored by adsorption calorimetry represent solely the binding of ethanol to the calcite surfaces.

Ethanol adsorption isotherms are shown in Fig. 1*A*. They are all type I isotherms (30) exhibiting steep initial uptake, an indication of strong chemisorption. Type I isotherm is observed when the adsorbate–adsorbent interaction is favorable yet the adsorption process features limited adsorbate layers (30). The adsorption amount varies for each sample due to their intrinsic geometric differences, including possible presence of pores and channels. We define differential enthalpy as the incremental change in molar enthalpy with increasing adsorption. The differential enthalpy of adsorption is plotted as function of the number of ethanol molecules adsorbed per nm^2 surface area (Fig. 1*B*). The initial dose of ethanol on fresh nanocalcite generates the most exothermic enthalpy of adsorption, −121.2 ± 2.4 kJ/mol ethanol. Further adsorption results in less exothermic heat effects. The differential enthalpy curve reaches its first plateau at −98.3 ± 4.8 kJ/mol ethanol, which spans 0.3–3.5 ethanol molecules per nm^2 (the latter being approximately a monolayer of ethanol), before ending with a sharp rise to the next plateau (−3.2 ± 1.6 kJ/mol ethanol) above 3.5 molecules per nm^2 (31). Surprisingly, the position of the second plateau is much less exothermic than that of the condensation enthalpy of ethanol [−42.3 kJ/mol, at 25 °C (32)]. This anomalous value suggests very weak interactions between this second layer of ethanol molecules and the calcite surface, among ethanol molecules in the second layer and/or between the first and second layer of adsorbate, such that the enthalpy of adsorption is much less exothermic than that associated with forming a normal liquid ethanol phase from the vapor. We define integral enthalpy of adsorption as the sum of differential adsorption enthalpies divided by the total moles of ethanol adsorbed up to certain coverage (Fig. 1*C*). It becomes less exothermic as adsorption proceeds, showing an inflection point at the same coverage as the sharp change on the differential enthalpy curve.

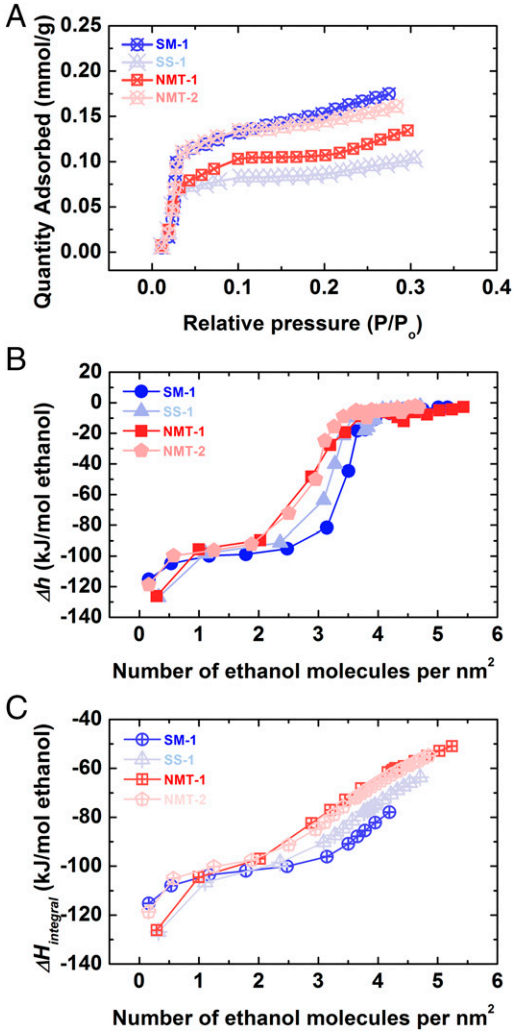

Fig. 1. (*A*) Ethanol adsorption isotherms, (*B*) corresponding differential, and (*C*) integral enthalpies of ethanol adsorption for nanophase calcite samples at 25 °C.

Discussion

This set of direct experimental observations enables us to understand the fundamental thermodynamics and surface chemistry for the ethanol–nanocalcite system. Strong thermochemical evidence linking the energetics and existence of a predicted spatially thin gap with low ethanol density (22) between the first adsorbed ethanol monolayer and the subsequent layer has been identified.

For each differential enthalpy curve, there appear to be three distinct sections: (*i*) the strong initial binding of ethanol on fresh nanocalcite, (*ii*) the intermediate chemisorption at the first plateau, and (*iii*) the weakest interaction at the second plateau. Our current work provides ethanol–nanocalcite binding energy at near-zero coverage (−121.2 ± 2.4 kJ/mol ethanol), which may not be readily calculated by fitting isotherms collected at various temperatures and has not, to our knowledge, been observed in previous investigations. Such strong adsorption usually happens on defect sites of NPs, which may be the atomic steps, corners (regions of high step density), or lattice defects (particularly impurities and vacancies), and perhaps plays a crucial role in the initiation of surface reaction between (bio)organic molecules and minerals. The first plateau at −98.3 ± 4.8 kJ per mole ethanol shows clear evidence of the formation of an approximately close-packed monolayer of ethanol with strong chemisorption at the nanocalcite surface. The termination of the first plateau at about 3.5 ethanol is in excellent agreement with the calculated monolayer coverage of ethanol on calcite, 3.6 molecules per nm^2 (31). Our results suggest that, regardless of their particle size or surface areas, different nanocalcites appear to have binding sites with quite similar energetic states. In addition, the current result on this plateau is in good accordance with both the simulated adsorption enthalpies (20), −91.3 [molecular mechanics (MM)] and −89.6 [density functional theory calculations (DFT)] kJ/mol ethanol, and the calculated isosteric heat (31) (−Qst, −94.0 kJ/mol ethanol). These strong interactions almost certainly arise from strong bonding between the calcite surface and the hydroxyl end of the ethanol molecule and guarantee robust connection at the interface, which may enable subtle tailoring of the surface properties (energy or charge or hydrophobicity), resulting in stable, controlled intermediate surfaces in organic ligand–NP reactions.

Calcite NP can be stabilized by adsorbed organic molecules; in return, the surface may also determine the configuration/microstructure of the bound adsorbates. Using MD simulation, Cooke et al. (21) predicted that ethanol was able to interact with both Ca–O and OH groups on the calcite surface, forming an ordered, very stable Langmuir adsorption monolayer. These conclusions were supported by AFM, showing that ethanol molecules self-assemble to a hydrophobic, new surface on calcite, which is even preserved in 50% ethanol aqueous solution (21). Later, Sand et al. (20) proposed that the highly ordered ethanol monolayer may be directed by the calcite surface. They also pointed out that once immersed in bulk ethanol, the calcite surface may impact the

molecular arrangement of bulk liquid phase for a significant distance. Furthermore, using coupled X-ray reflectivity and MD, Pasarín et al. (22) described a more detailed surface configuration with a highly ordered ethanol monolayer about 6 Å in height forming at the ethanol–calcite interface, and a subsequent thin gap of about 1 Å indicated by an extremely low density of ethanol. This gap is then followed by a region of more disordered layers about 14 Å, mostly with their hydrophobic ends pointing toward the gap. Recently, the binding energies between alcohols and calcium carbonate phases were studied using both DFT and isosteric heat calculation (Q_{st}) from adsorption isotherm data between 0 and 20 °C. It was found that alcohols heavier than methanol (including ethanol) tend to bind to the calcite surface more strongly than water and acetic acid (31). Very recently, the interactions of a series of alcohols with the calcite surface were studied using X-ray photoelectron spectroscopy coupled with MD simulation, in which all alcohols were found to bond with calcite surface through the hydroxyl group forming closely packed, ordered monolayer (33). All these previous investigations suggest a spatially thin gap with low ethanol density between the first adsorbed monolayer and the bulk alcohol. Our thermodynamic study strongly supports such a model (22). Specifically, the first ethanol monolayer constructs a hydrophobic new surface with its $–CH_3$ tail facing outward, indicated by the second plateau on the differential enthalpy profile, with near-zero physisorption enthalpy. In this circumstance, the ethanol molecules immediately beyond this gap cannot form effective bonding with the hydrophobic tails of the monolayer of ethanol, whose hydrophilic ends are inaccessible, being tethered to the calcite surface. Indeed, a recent X-ray pair distribution function analysis study suggested that such enhanced short-range order of organic molecules, both polar and nonpolar, induced by colloidal NPs is universal. The restructuring effect may reach up to 2 nm beyond the particle surface and directly contribute to the functionality of NPs (34).

Water is the most common adsorbate on NP surfaces and it may compete with organics and affect the ligand–NP reactions. Despite the same functional group (hydroxyl, –OH), the adsorption enthalpies for water and ethanol exhibit distinct behavior (Fig. 2). Unlike ethanol, water adsorption generates type II isotherms (30) with more positive slope and higher uptake throughout all P/P_o range ($P_{o\text{-water}}$ = 23.77 mm Hg and $P_{o\text{-ethanol}}$ = 58.75 mm Hg, at 25 °C). In addition to favorable adsorption, the type II isotherm also suggests continuous formation of water multilayers until saturation (30). At near-zero coverage, adsorption of both molecules on a fresh nanocalcite surface produces a very similar heat effect (Fig. 2*B*). This probably reflects the energetic states of the surface defects of nanocalcite, which may be able to accommodate the OH group from water or from ethanol with similar energetics. As coverage increases, differential enthalpies of both water and ethanol adsorption become less exothermic. However, unlike the differential enthalpy profile of ethanol adsorption, water adsorption merely shows a single differential enthalpy plateau at its heat of condensation (−44.0 kJ/mol). Hence, the adsorption energy differences clearly distinguish the discontinuity of ethanol adsorption from the continuity for water layers on nanocalcite. The integral enthalpy of adsorption leads to the same conclusion by showing a clear discontinuity in slope for ethanol at about 3.5 molecules per nm^2, whereas the trend for water adsorption appears continuous and monotonic. Moreover, at any particular partial pressure (P/P_o) below 0.05, the binding of ethanol is more exothermic than that of water (Fig. S1). Interestingly, analogous adsorption behavior has also been observed on mesoporous silica, with ethanol showing much stronger binding with the surface than water (35).

We also calculated the partial molar free energy (chemical potential) and entropy change ($\Delta\mu$ and Δs) plots for both vapors (Fig. 3). The selected equilibrium system includes both gas-phase

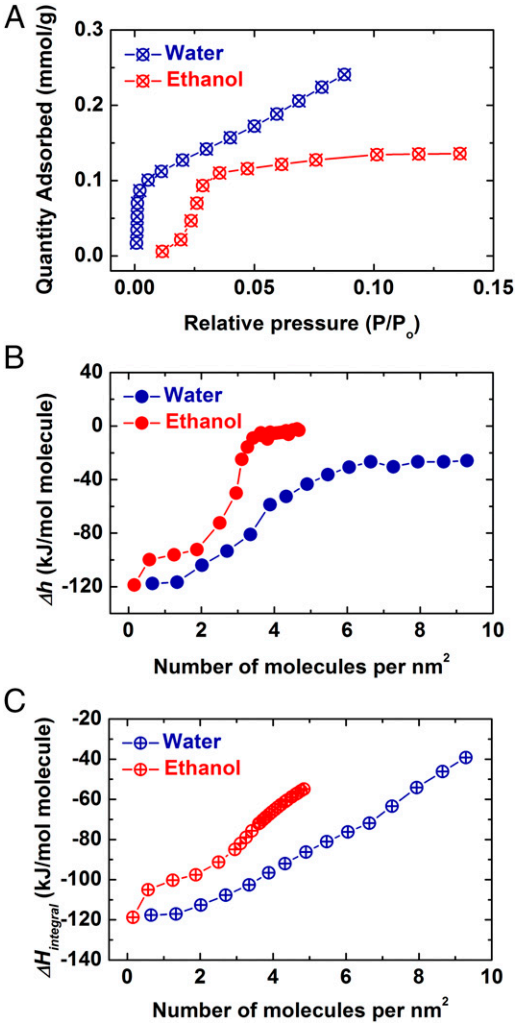

Fig. 2. (*A*) Water and ethanol adsorption isotherms, (*B*) corresponding differential, and (*C*) integral enthalpies of adsorption for the nanophase calcite NMT-2, at 25 °C. The water adsorption calorimetry data for NMT-2 are reproduced from ref. 29.

and surface-adsorbed ethanol molecules in the forked tube. Pure gas phase (water or ethanol) at 1 atm and 25 °C was selected as the standard state. The $\Delta\mu$ was derived directly from the adsorption isotherm [$\Delta\mu = RT\ \ln(p/p_o)$, p_o = 1 atm], and Δs is calculated by the equation $\Delta\mu = \Delta h - T\Delta s$. The $\Delta\mu$ and Δs curves mimic the fashion of Δh, both of which become less negative as more molecules are adsorbed, stepwise for ethanol and gradually for water. Interestingly, upon monolayer formation, the trend of chemical potential plot of ethanol adsorption strongly suggests great depression of affinity on an energetically less favorable surface of carbon tails, indicated by the second, near-zero plateau (Fig. 3*A*), and supported by the positive values of entropy change (Fig. 3*B*). On the other hand, all partial molar properties of water–calcite NP interactions suggest steady adsorption with continuous formation of stacked water multilayers.

The calorimetric data on NPs support and provide a quantitative energetic basis for the structural observations, many of which refer to the surface of bulk calcite or to idealized surfaces. This agreement suggests that the defect density (steps, kinks, chemical defects) on the relatively large NPs we studied is not high enough to significantly disrupt the ordering of ethanol molecules on the NP surfaces. Smaller particles, which appear

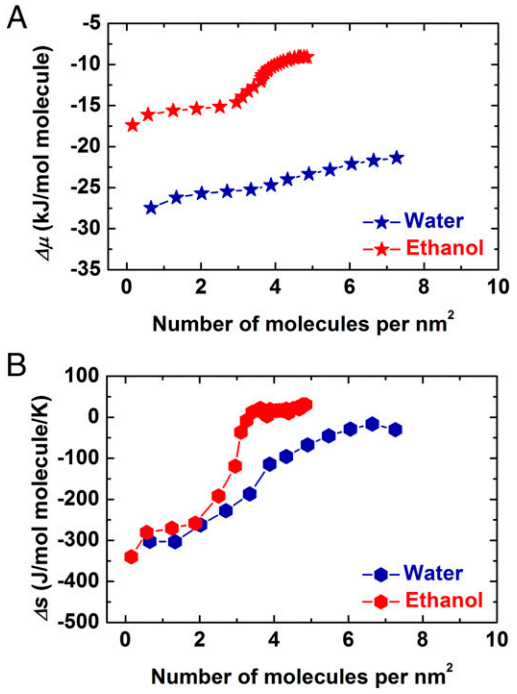

Fig. 3. (*A*) Free energies and (*B*) differential entropies of water (blue) and ethanol (red) adsorption at 25 °C on NMT-2.

very difficult to make without strongly bonded organic capping agents, may adsorb ethanol differently.

The current thermodynamic investigation provides crucial insights on organic ligand–NP interactions for geological and technological systems as illustrated below. First, the tight capping of organic ligands may shield the NP from harsh environments. In other words, the strong exothermic binding observed in the present work may effectively counteract the inherent high surface energy of bare inorganic NP, paying for the energy cost of "being exceptionally small." For instance, it is found that the adsorbed organics (mainly proteins) generated by microorganisms may significantly stabilize the highly metastable precursor phases in biologically controlled mineralization and early stages of geologic CO_2 sequestration, to achieve delicate development of crystals with preferred sizes and morphologies (36–38). Such natural strategies are mirrored in the synthesis of artificial colloidal NPs. Upon organic ligand assembly, the newly formed hydrophobic soft shell surface may not only significantly lower the surface energy, disperse the NPs uniformly in different organic solvents, but also ensure formation of a monodisperse array of colloidal NPs, with defined phase, shape, and size (12, 39). Therefore, these observations further suggest that subtle manipulation of the interplay of thermodynamic driving force and surface chemistry may hold the key to rational design of stable materials or devices at the nanoscale.

Strong interactions at the ligand–NP interfaces create thermodynamically stable hybrid core–shell nanostructures, which often feature selectivity and reactivity that can be optimized for specific functions. Indeed, such delicate functionality is directly linked to the evolved free energy owing to organic capping. For example, the protein monolayer-coated NPs appear to have hydrophobic surfaces and may selectively bind other biological entities (proteins/enzymes/DNA and cells), making effective biomolecular transporters and/or sensors (37, 40). Interestingly, similar selective molecular recognition is also seen in engineered hydrogenation reactions using alkylamine-capped NP catalysts, wherein substantially enhanced catalytic selectivity has been reported. Stereo-, electro-, and chemical-selective controls are discussed (7). The energetics of ligand binding as well as its coverage are crucial factors governing the reactivity and selectivity. Capping ligands binding too weakly may have little or no effect on selectivity. However, if they are bonded too tightly, the ligand capping may significantly reduce the catalytic activity. Using NMR spectroscopy, Valdez et al. (41) recently demonstrated that the capping of dodecylamine on zinc oxide NPs was patchy, including three types of binding: strongly bound, weakly associated, and free molecules in solution. The capping group density was also quantified, however, the magnitude of different interactions has not been determined. Our measurements demonstrate accurate quantification of ligand–NP interaction at the interface. Furthermore, we argue that such stepwise energetic profiles may be common for ligand–NP binding, especially if the inorganic core is small and with various defined facets, which may interact differently with the same ligand or selectively bind specific organic molecules. Although the energetics of ligand–NP interaction may appear in a stepwise fashion, the gradual transition from weakly bonded exchangeable surface layer to strongly bonded to classical capping is a continuum and not a set of different phenomena. Accurate quantification of such ligand–NP interactions may be successfully performed by careful design of calorimetric experiments in appropriate conditions. Although we did not study the kinetics of the displacement of water by ethanol and other molecules, it is clear that such work would be valuable for both geochemical and materials applications. The thermodynamics of these interactions, which was our focus, must be the starting point for kinetic and mechanistic studies.

The conditions for underground CO_2 sequestration represent another "harsh environment." It is impossible at present to reliably extrapolate our calorimetric adsorption data for water, CO_2, or ethanol to conditions of supercritical CO_2. Nevertheless, our data represent a starting point which may be especially useful for molecular modeling approaches to the sequestration environment. The competition among CO_2, water, and organics for binding to mineral surfaces and to each other under such conditions clearly needs detailed study in terms of both thermodynamics and kinetics.

Conclusion

Using direct gas adsorption calorimetry, we clearly demonstrated strong bonding for the formation of an ethanol monolayer on the nanocalcite surface. The existence of a low-density gap between the first and second layer of adsorbed ethanol is strongly supported by the thermochemical data. In a broader sense, knowing such small organic molecule–NP interaction is a crucial first step to understand much more complicated organic ligand–inorganic NP interactions at the interfaces in both natural geological and biological environments and technological conditions. Moreover, the fundamental thermodynamic information may offer valuable insights and aids to material scientists for rational design and fabrication of advanced (bio)hybrid nanoscale functional materials.

Materials and Methods

The enthalpies of ethanol adsorption were measured by a gas adsorption calorimetry system, which included a Calvet-type microcalorimeter (Setaram Sensys) coupled to a gas adsorption analyzer (Micromeritics ASAP 2020), as described previously (25). Specifically, hand-pressed sample pellet with about 5 m^2 total surface area was loaded into one side of a silica glass forked tube, the other side of which was left empty acting as reference. The tube was inserted into the twin chambers of the microcalorimeter, connected to the analysis port of the ASAP 2020, and subjected to strong vacuum degas ($<10^{-3}$ Pa) at 150 °C for 6 h to remove all adsorbed species. The ASAP 2020 was operated in incremental dosing mode (1 μmol) with a reaction equilibration time of 1.0 h. Each dose of ethanol (pure, anhydrous alcohol, Fluka) vapor produces a distinct calorimetric signal whose area represents the heat of adsorption and the amount adsorbed was determined by the pressure drop at equilibrium.

ACKNOWLEDGMENTS. We thank Sergey V. Ushakov and Krasen Kovachev for technical support. We also thank Susan Stipp and her group and Zewei Quan for discussion. The calorimetric work was supported by the US Department of Energy, Office of Basic Energy Sciences, Grant DE-FG02-97ER14749.

1. Subburaman K, et al. (2006) Templated biomineralization on self-assembled protein fibers. *Proc Natl Acad Sci USA* 103(40):14672–14677.
2. Theng BKG, Yuan GD (2008) Nanoparticles in the soil environment. *Elements* 4(6): 395–399.
3. Radha AV, Forbes TZ, Killian CE, Gilbert PUPA, Navrotsky A (2010) Transformation and crystallization energetics of synthetic and biogenic amorphous calcium carbonate. *Proc Natl Acad Sci USA* 107(38):16438–16443.
4. Elhadj S, De Yoreo JJ, Hoyer JR, Dove PM (2006) Role of molecular charge and hydrophilicity in regulating the kinetics of crystal growth. *Proc Natl Acad Sci USA* 103(51):19237–19242.
5. Hamm LM, et al. (2014) Reconciling disparate views of template-directed nucleation through measurement of calcite nucleation kinetics and binding energies. *Proc Natl Acad Sci USA* 111(4):1304–1309.
6. Daniel MC, Astruc D (2004) Gold nanoparticles: Assembly, supramolecular chemistry, quantum-size-related properties, and applications toward biology, catalysis, and nanotechnology. *Chem Rev* 104(1):293–346.
7. Kwon SG, et al. (2012) Capping ligands as selectivity switchers in hydrogenation reactions. *Nano Lett* 12(10):5382–5388.
8. Okrut A, et al. (2014) Selective molecular recognition by nanoscale environments in a supported iridium cluster catalyst. *Nat Nanotechnol* 9(6):459–465.
9. Crossley S, Faria J, Shen M, Resasco DE (2010) Solid nanoparticles that catalyze biofuel upgrade reactions at the water/oil interface. *Science* 327(5961):68–72.
10. Pang X, Zhao L, Han W, Xin X, Lin Z (2013) A general and robust strategy for the synthesis of nearly monodisperse colloidal nanocrystals. *Nat Nanotechnol* 8(6):426–431.
11. Baghbanzadeh M, Carbone L, Cozzoli PD, Kappe CO (2011) Microwave-assisted synthesis of colloidal inorganic nanocrystals. *Angew Chem Int Ed Engl* 50(48):11312–11359.
12. Murray CB, et al. (2001) Colloidal synthesis of nanocrystals and nanocrystal superlattices. *IBM J Res Develop* 45(1):47–56.
13. Liang X, et al. (2014) Synthesis of unstable colloidal inorganic nanocrystals through the introduction of a protecting ligand. *Nano Lett* 14(6):3117–3123.
14. Lin KYA, Park AHA (2011) Effects of bonding types and functional groups on CO2 capture using novel multiphase systems of liquid-like nanoparticle organic hybrid materials. *Environ Sci Technol* 45(15):6633–6639.
15. Tang R, et al. (2005) Control of biomineralization dynamics by interfacial energies. *Angew Chem Int Ed Engl* 44(24):3698–3702.
16. Li XL, et al. (2014) Templated biomineralization on self-assembled protein nanofibers buried in calcium oxalate raphides of Musa spp. *Chem Mater* 26(12):3862–3869.
17. Cartwright JHE, Checa AG, Gale JD, Gebauer D, Sainz-Díaz CI (2012) Calcium carbonate polyamorphism and its role in biomineralization: How many amorphous calcium carbonates are there? *Angew Chem Int Ed Engl* 51(48):11960–11970.
18. Addadi L, Weiner S (1992) Control and design principles in biological mineralization. *Angew Chem Int Ed Engl* 31(2):153–169.
19. Nudelman F, Sommerdijk NAJM (2012) Biomineralization as an inspiration for materials chemistry. *Angew Chem Int Ed Engl* 51(27):6582–6596.
20. Sand KK, et al. (2010) Binding of ethanol on calcite: The role of the OH bond and its relevance to biomineralization. *Langmuir* 26(19):15239–15247.
21. Cooke DJ, Gray RJ, Sand KK, Stipp SLS, Elliott JA (2010) Interaction of ethanol and water with the 1014 surface of calcite. *Langmuir* 26(18):14520–14529.
22. Pasarín IS, et al. (2012) Molecular ordering of ethanol at the calcite surface. *Langmuir* 28(5):2545–2550.
23. Navrotsky A, Mazeina L, Majzlan J (2008) Size-driven structural and thermodynamic complexity in iron oxides. *Science* 319(5870):1635–1638.
24. Navrotsky A, Ma C, Lilova K, Birkner N (2010) Nanophase transition metal oxides show large thermodynamically driven shifts in oxidation-reduction equilibria. *Science* 330(6001):199–201.
25. Ushakov SV, Navrotsky A (2005) Direct measurements of water adsorption enthalpy on hafnia and zirconia. *Appl Phys Lett* 87(16):164103.
26. Wu D, et al. (2013) Direct calorimetric measurement of enthalpy of adsorption of carbon dioxide on CD-MOF-2, a green metal-organic framework. *J Am Chem Soc* 135(18):6790–6793.
27. Gouvêa D, Ushakov SV, Navrotsky A (2014) Energetics of CO_2 and H_2O adsorption on zinc oxide. *Langmuir* 30(30):9091–9097.
28. Hulvey Z, et al. (2013) Noble gas adsorption in copper trimesate, HKUST-1: An experimental and computational study. *J Phys Chem C* 117(39):20116–20126.
29. Forbes TZ, Radha AV, Navrotsky A (2011) The Energetics of Nanophase Calcite. *Geochim Cosmochim Acta* 75(24):7893–7905.
30. Lowell S (2006) *Characterization of Porous Solids and Powders: Surface Area, Pore Size, and Density* (Springer, Dordrecht, The Netherlands), p xiv.
31. Okhrimenko DV, Nissenbaum J, Andersson MP, Olsson MHM, Stipp SLS (2013) Energies of the adsorption of functional groups to calcium carbonate polymorphs: The importance of -OH and -COOH groups. *Langmuir* 29(35):11062–11073.
32. Dionisio MS, Ramos JJM, Goncalves RM (1990) The enthalpy and entropy of cavity formation in liquids and corresponding states principle. *Can J Chem* 68(11):1937–1949.
33. Bovet N, Yang M, Javadi MS, Stipp SLS (2015) Interaction of alcohols with the calcite surface. *Phys Chem Chem Phys* 17(5):3490–3496.
34. Zobel M, Neder RB, Kimber SAJ (2015) Universal solvent restructuring induced by colloidal nanoparticles. *Science* 347(6219):292–294.
35. Wu D, Navrotsky A (2013) Small molecule - silica interactions in porous silica structures. *Geochim Cosmochim Acta* 109:38–50.
36. Barroso da Silva FL, Boström M, Persson C (2014) Effect of charge regulation and ion-dipole interactions on the selectivity of protein-nanoparticle binding. *Langmuir* 30(14):4078–4083.
37. Mahmoudi M, et al. (2011) Protein-nanoparticle interactions: opportunities and challenges. *Chem Rev* 111(9):5610–5637.
38. Lynch I, Dawson KA (2008) Protein-nanoparticle interactions. *Nano Today* 3(1-2): 40–47.
39. Quan ZW, Fang JY (2010) Superlattices with non-spherical building blocks. *Nano Today* 5(5):390–411.
40. Monopoli MP, Aberg C, Salvati A, Dawson KA (2012) Biomolecular coronas provide the biological identity of nanosized materials. *Nat Nanotechnol* 7(12):779–786.
41. Valdez CN, Schimpf AM, Gamelin DR, Mayer JM (2014) Low capping group surface density on zinc oxide nanocrystals. *ACS Nano* 8(9):9463–9470.